Hydrometeorological application of a microwave link: 1. Evaporation

H. Leijnse,[1] R. Uijlenhoet,[1] and J. N. M. Stricker[1]

Received 21 February 2006; revised 31 May 2006; accepted 23 August 2006; published 12 April 2007.

[1] A method to estimate areal evaporation using a microwave link (radio wave scintillometer) in combination with an energy budget constraint is proposed. This radio wave scintillometry-energy budget method (RWS-EBM) is evaluated for its applicability in different meteorological conditions and for its sensitivity to various variables (the structure parameter of the refractive index of air C_n^2, the total available energy $R_n - G$, the wind velocity u, the effective average vegetation height h_0, and the correlation coefficient between the temperature and humidity fluctuations r_{TQ}). The method is shown to be best suited for use in wet to moderately dry conditions, where the latent heat flux is at least a third of the total available energy (i.e., Bowen ratio ≤ 2). It is important to accurately measure the total available energy and the wind velocity as the RWS-EBM is most sensitive to these variables. The Flevoland field experiment has provided the data, obtained with a 27-GHz radio wave scintillometer (over 2.2 km), a large-aperture scintillometer (also 2.2 km), and four eddy covariance systems, which are used to test the RWS-EBM. Comparing 92 daytime measurements (30-min intervals) of the evaporation estimated using the RWS-EBM to that determined in alternative manners (eddy covariance and two-wavelength scintillometry) leads to the conclusion that the method provides consistent estimates (coefficient of determination $r^2 = 0.85$ in both cases) under relatively wet conditions.

Citation: Leijnse, H., R. Uijlenhoet, and J. N. M. Stricker (2007), Hydrometeorological application of a microwave link: 1. Evaporation, *Water Resour. Res.*, *43*, W04416, doi:10.1029/2006WR004988.

1. Introduction

[2] The objective of our work is to show that single-frequency microwave links offer the potential to measure both path-averaged evaporation and precipitation (see Figure 1). In the present paper, the possibilities and restrictions of a microwave link for measuring evaporation are investigated. The measurement of precipitation using a microwave link is discussed by *Leijnse et al.* [2007].

[3] Areal evaporation is an important component of the exchanges of water and energy between the land surface and the atmosphere. Therefore accurate knowledge of its spatial and temporal variability is crucial for improving hydrological, meteorological and climate models [e.g., *Parlange et al.*, 1995]. Nowadays the estimation of actual evaporation is usually carried out by measuring turbulence statistics at local scales (eddy covariance (EC) method [e.g., *Brutsaert*, 1982]), whereas at larger scales highly intermittent, pixel-averaged satellite observations [*Bastiaanssen*, 2000; *Bastiaanssen et al.*, 2002; *Su*, 2002] are used. Scintillometers could potentially complement these types of measurements. *Meijninger et al.* [2002a] have shown that scintillometers are relatively insensitive to modest land use heterogeneities. Thus they provide a greater spatial representation of evaporative flux measurements than point-scale methods like, for example, the EC method. The integrated scales at which scintillometers operate correspond nicely to the grid scales of satellite-based retrieval algorithms of the evaporative flux. As a consequence, scintillometer measurements may be used as a reference and as validation for these algorithms.

[4] In the recent literature on scintillometry, the emphasis has been on the use of optical or infrared instruments, which, in contrast to microwave scintillometers, measure mainly the sensible heat flux. For example, a recent special issue on scintillometry (see editorial by *de Bruin* [2002]) contained nine papers, of which only one [*Meijninger et al.*, 2002b] deals with microwave scintillometry, in this case in combination with large-aperture (optical) scintillometry. A similar combination of scintillometer frequencies was used by *Green et al.* [2000, 2001]. Less recently, *Kohsiek and Herben* [1983] have successfully used a stand-alone radio wave scintillometer to estimate evaporation using several simplifying assumptions. Here, we focus on a stand-alone radio wave scintillometer because of its potential for simultaneously measuring precipitation [see *Leijnse et al.*, 2007].

[5] A scintillometer consists of a transmitter and a receiver, typically at a distance of several hundred meters up to a few kilometers, and at a height well inside the surface layer of the atmosphere. The signal propagates through this turbulent atmospheric surface layer, of which the general structure is well established [e.g., *Pope*, 2000]. Local temperature and humidity variations caused by the turbulent eddies produce refractive index fluctuations which in turn

[1] Hydrology and Quantitative Water Management, Wageningen University, Wageningen, Netherlands.

0043-1397/07/2006WR004988$09.00

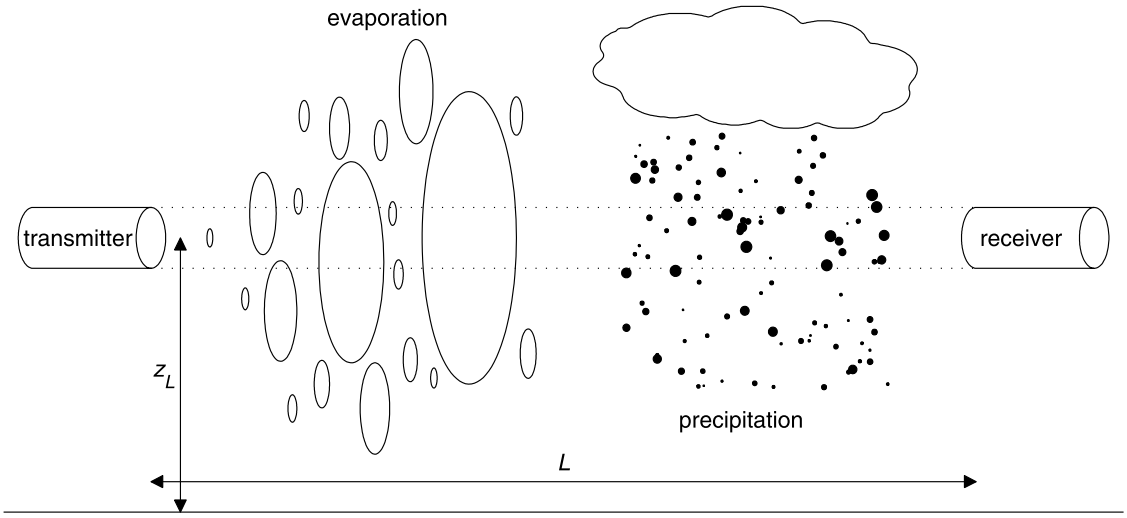

Figure 1. The microwave link setup. Turbulent eddies are depicted as ellipses on the left, and precipitation is shown on the right.

cause the electromagnetic signal to scintillate. In Figure 1, the refractive index variations in the turbulent eddies are depicted as lenses which cause refraction of the signal. The rain in Figure 1 is shown merely to indicate the potential of the instrument for measuring precipitation. Assuming statistical stationarity, the turbulence intensity averaged over a certain time interval can be described using a so-called structure parameter. The structure parameter of the refractive index of air can be determined by recording the variance of the scintillometer signal at the receiver. Because the refractive index of air is a function of temperature and humidity, the sensible (temperature related) and latent (humidity related) heat fluxes determine the value of this structure parameter. This implies that both heat fluxes can in principle be estimated from the microwave scintillometer signal given an additional constraint. The evaporation E (kg m^{-2} s^{-1}) is directly related to the latent heat flux L_vE (W m^{-2}) through the latent heat of vaporization of water L_v ($\approx$2.453 $\times$ 10^6 J kg^{-1}). *Meijninger et al.* [2002b] obtained good results with a microwave scintillometer using a large-aperture (optical) scintillometer (which is mainly sensitive to temperature fluctuations, and thus the sensible heat flux) to provide the necessary additional constraint. We use measurements of the total available energy and the surface energy budget to provide this constraint.

[6] In this paper, a method is presented to estimate the sensible and latent heat fluxes (and hence the evaporation) using a microwave link (or a radio wave scintillometer) with the surface energy budget constraint. This method will be presented in section 2, after which its applicability in different conditions will be discussed in section 3. Data obtained with a 27-GHz scintillometer, collected during the Flevoland field experiment [*Meijninger et al.*, 2002a, 2002b], is used to test the method experimentally in section 4, and conclusions will be drawn in section 5.

2. Radio Wave Scintillometry-Energy Budget Method

[7] The quantity that is calculated from the scintillometer signal is the variance of the natural logarithm of the signal intensity at the receiver. This variance is a function of the structure parameter of the refractive index of air C_n^2 (m$^{-2/3}$), which, at radio wave frequencies, depends on the structure parameters of temperature and humidity. These relations will be discussed in section 2.1. The structure parameters of temperature and humidity are in turn related to the sensible and latent heat fluxes through the Monin-Obukhov similarity theory (MOST), which will be discussed in section 2.2. The surface energy budget is used to constrain the heat fluxes derived from the scintillometer measurements. This radio wave scintillometry-energy budget method (RWS-EBM) will be presented in section 2.3.

2.1. Principle of Scintillometry

[8] *Tatarskii* [1971] has derived a relation between the variance of the natural logarithm of the intensity of a signal with wavelength λ (m) originating from a point source (spherical wave) $\sigma^2_{\ln(I)}$ and the structure parameter of the refractive index of the air between the point source and the receiver

$$C_n^2 = \frac{2^{14/3}\Gamma\left(\frac{7}{3}\right)\cos\left(\frac{\pi}{12}\right)}{\pi\sqrt{3\pi}\Gamma\left(\frac{8}{3}\right)} k^{-7/6} L^{-11/6} \sigma^2_{\ln(I)}, \tag{1}$$

where $\Gamma()$ is the gamma function, k (= $2\pi/\lambda$) is the wave number of the signal and L (m) is the length of the link.

[9] The refractive index of air n (dimensionless) is affected by that of dry air, the water vapor present in this air, and the proximity of the signal frequency to an absorption line of water vapor. As a result it depends on the temperature T (K), the absolute humidity Q (kg m^{-3}) and the pressure p (Pa) of the air. *Hill et al.* [1980] give a relation between the structure parameter of the refractive index of air and the structure parameters of temperature C_T^2 (K^2 m$^{-2/3}$) and moisture C_Q^2 (kg^2 m$^{-20/3}$)

$$C_n^2 = A_T^2 \frac{C_T^2}{T^2} + A_Q^2 \frac{C_Q^2}{Q^2} + 2A_T A_Q \frac{C_{TQ}}{TQ}, \tag{2}$$

where the contribution due to pressure fluctuations is neglected. Following the suggestion by *Kohsiek and Herben*

[1983], the cross-structure parameter of temperature and humidity C_{TQ} (K kg m$^{-11/3}$) can be written as $C_{TQ} = r_{TQ}C_TC_Q$, in which r_{TQ} is the correlation coefficient between the temperature and humidity fluctuations. The dimensionless sensitivity coefficients of the refractive index A_T and A_Q at radio wavelengths longer than 3 mm are given by *Andreas* [1989]

$$A_T = T\frac{\partial n}{\partial T} = -b\frac{p}{T} - c\frac{Q}{T} \tag{3}$$

$$A_Q = Q\frac{\partial n}{\partial Q} = c\frac{Q}{T} \tag{4}$$

[see also *Hill and Clifford*, 1981], with $b = 0.776 \times 10^{-6}$ K Pa^{-1} and $c = 1.723$ K m^3 kg^{-1}.

2.2. Monin-Obukhov Similarity Theory

[10] The Monin-Obukhov similarity theory is valid in the surface layer of the atmosphere and describes the profiles of momentum and conservative scalars. It is theoretically only valid over homogeneous terrain, but, as stated by *Meijninger et al.* [2002b], the effect of heterogeneity is small. MOST can be used to relate the structure parameters C_T^2 and C_Q^2 at a given height in the surface layer to the sensible (H_s) and latent (L_vE) heat fluxes (both in W m^{-2})

$$\frac{\rho^2 c_p^2 C_T^2}{H_s^2} = \frac{L_v^2 C_Q^2}{(L_vE)^2} = \frac{1}{u_*^2 (z_L - d_0)^{2/3}} f_{Ob}\left(\frac{z_L - d_0}{L_{Ob}}\right), \tag{5}$$

where the specific heat of air at constant pressure is $c_p \approx 1005$ J kg^{-1} K^{-1}, u_* (m s^{-1}) is the friction velocity, z_L (m) is the height above the terrain, d_0 (m) is the displacement height of the turbulent boundary layer. The Obukhov length L_{Ob} (m) is a measure of the stability of the surface layer, and will be discussed later. The density of moist air ρ (kg m^{-3}) is given by

$$\rho = \frac{p}{R_d T} - 0.61Q \tag{6}$$

[e.g., *Brutsaert*, 1982], where R_d (≈ 287.04 J kg^{-1} K^{-1}) is the gas constant of dry air.

[11] The main focus of this paper will be on estimating evaporation. Because the evaporation is directly related to the latent heat flux, the analyses presented here will concern only the latent heat flux explicitly. The sensible heat flux can easily be computed from this using the surface energy budget. As evaporation occurs predominantly during the daytime, we only consider unstable atmospheric conditions and, correspondingly, only positive (i.e., upward) heat fluxes.

[12] The shape of f_{Ob} can be derived from the relations given by *Businger et al.* [1971]. For unstable conditions ($L_{Ob} < 0$ m), this function is

$$f_{Ob}\left(\frac{z_L - d_0}{L_{Ob}}\right) = c_1\left(1 - c_2\frac{z_L - d_0}{L_{Ob}}\right)^{-2/3}. \tag{7}$$

The constants $c_1 = 4.9$ and $c_2 = 7.0$ were empirically derived for C_T^2 profiles by *Wyngaard et al.* [1971]. *Andreas* [1988] later corrected the second constant to be $c_2 = 6.1$ to take into account the new value of the von Kármán constant κ (= 0.4; *Wyngaard et al.* [1971] assumed $\kappa = 0.35$). An alternative expression exists for stable conditions, which is not used here because it falls outside the scope of the current paper. The Obukhov length is given by [e.g., *Brutsaert*, 1982]

$$L_{Ob} = -\frac{\rho u_*^3}{\kappa g\left(\frac{1}{c_pT}H_s + \frac{0.61}{L_v}L_vE\right)}, \tag{8}$$

where g is the acceleration of gravity (≈ 9.81 m s^{-2}) and κ is the von Kármán constant (≈ 0.4). Given a wind velocity u (m s^{-1}) measured at a height above the terrain z_u (m), the friction velocity can be calculated using

$$u_* = \frac{\kappa u}{\ln\left(\frac{z_u - d_0}{z_0}\right) - \Psi\left(\frac{z_u - d_0}{L_{Ob}}\right) + \Psi\left(\frac{z_0}{L_{Ob}}\right)} \tag{9}$$

[e.g., *Brutsaert*, 1982], where z_0 (m) is the momentum roughness length of the terrain, and Ψ is the Businger-Dyer expression

$$\Psi\left(\frac{z}{L_{Ob}}\right) = 2\ln\left(\frac{1+x}{2}\right) + \ln\left(\frac{1+x^2}{2}\right) - 2\arctan(x) + \frac{\pi}{2}, \tag{10}$$

with

$$x = \left(1 - 16\frac{z}{L_{Ob}}\right)^{1/4}. \tag{11}$$

These empirical relations have been shown to be valid in the range $-\frac{z}{L_{Ob}} \lesssim 2$.

[13] The roughness length z_0 and the displacement height d_0 both depend on the height, the spacing and the shape of upwind obstacles in the field. For nonsparse vegetation, *Brutsaert* [1982] relates these parameters to the average height of the obstacles h_0 (m) according to

$$z_0 = \frac{1}{8}h_0 \tag{12}$$

$$d_0 = \frac{2}{3}h_0. \tag{13}$$

In an extensive literature review, *Wieringa* [1992] has tabulated z_0 as a function of terrain type. Equations (12) and (13) can be used to compute d_0 from this roughness length. The independent quantity that will be used in the remainder of this paper will be h_0.

2.3. Energy Budget Constraint

[14] The system of equations presented in section 2.2 can be closed by using the principle of conservation of energy, which requires the sum of the latent and sensible heat fluxes to be equal to the total available energy

$$L_vE + H_s = R_n - G, \tag{14}$$

where R_n (W m^{-2}) is the net radiation and G (W m^{-2}) is the ground heat flux (both positive when downward). For

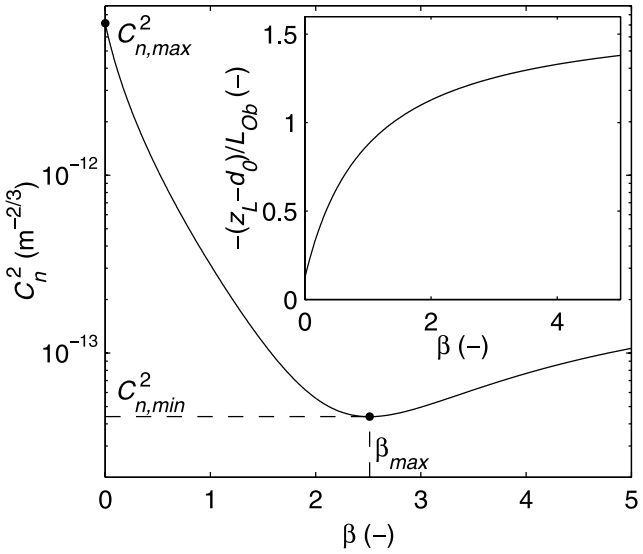

Figure 2. C_n^2 and $-\frac{z_L-d_0}{L_{Ob}}$ as functions of β, for $R_n - G$ = 400 W m^{-2}, u = 3.0 m s^{-1}, h_0 = 0.5 m, and r_{TQ} = 0.9.

convenience we use the Bowen ratio, defined as the ratio of the sensible and latent heat fluxes, as the variable to be computed

$$\beta = \frac{H_s}{L_v E}. \tag{15}$$

Both heat fluxes can then be computed from β using $R_n - G$ and equation (14)

$$H_s = \frac{\beta}{1+\beta}(R_n - G) \tag{16}$$

$$L_v E = \frac{1}{1+\beta}(R_n - G). \tag{17}$$

[15] With the energy budget (equation (14)), the number of equations (four: equations (2), (5), and (14), where equation (5) represents two equations) equals the number of unknowns (four: C_T^2, C_Q^2, H_s and L_vE) so that the Bowen ratio (and hence the turbulent fluxes) can in principle be solved, albeit implicitly. As an example, Figure 2 shows the $C_n^2(\beta)$ relation for $R_n - G$ = 400 W m^{-2}, u = 3.0 m s^{-1}, h_0 = 0.5 m and r_{TQ} = 0.9. The pressure, temperature and humidity are taken as constants here and in section 3 (p = 101.3 kPa, T = 288.15 K, Q = 0.015 kg m^{-3}), as changes in these variables do not greatly affect results. The height of the scintillometer and the height of the wind velocity measurements are also constant in the remainder of this paper. Their values (z_L = 10.9 m and z_u = 3.9 m) correspond to those of the experimental setup described in section 4. Figure 2 also shows that the value of $-\frac{z_L-d_0}{L_{Ob}}$ is within the range of validity of MOST.

3. Applicability

[16] As can be seen from Figure 2, the solution of the system of equations presented in the previous section does not exist for all values of C_n^2, and is not unique in the range where it does exist. This will be discussed in section 3.1. It can also be seen from Figure 2 that the solution is much more sensitive to changes (or errors) in C_n^2 for higher values of β (dry conditions) than for low values of β (wet conditions). An analysis of the sensitivity of the method to different variables will be given in section 3.2. Factors that may introduce errors in the estimated evaporative flux are discussed in section 3.3.

3.1. Region of Validity

[17] For a certain range of values of C_n^2, the system of equations presented in section 2 has multiple solutions. As radio wave scintillometers are influenced more by humidity fluctuations (related to the latent heat flux) than by temperature fluctuations (associated with the sensible heat flux), this type of instrument is best suited for wet to moderately dry conditions. Therefore we will consider only the solution in the region $\beta < \beta_{\max}$ (see Figure 2).

[18] Figure 2 shows that $\frac{\partial C_n^2}{\partial \beta}$ is negative in the region $\beta < \beta_{\max}$. This means there is a physical constraint on the value of C_n^2 (which has a maximum at β = 0). When β approaches 0, L_vE approaches $R_n - G$ and C_n^2 approaches $\frac{A_Q^2}{Q^2}C_Q^2$, which implies (see equation (5))

$$C_n^2 \le C_{n,\max}^2 = \frac{c_1 (R_n - G)^2 A_Q^2}{L_v^2 u_*^2 (z_L - d_0)^{2/3} Q^2} \times \left(1 - c_2 \frac{z_L - d_0}{L_{Ob}}\right)^{-2/3}, \tag{18}$$

where L_{Ob} (see equation (8)) now reduces to

$$\lim_{\beta \to 0} L_{Ob} = -\frac{\rho L_v u_*^3}{0.61 \kappa g (R_n - G)}. \tag{19}$$

[19] Unfortunately, there is no simple analytical expression for $\beta_{\max}$ or $C_{n,\min}^2$. However, when $r_{TQ} = \pm 1$, equation (2) can be rewritten using equation (5)

$$C_n^2 = \left(\frac{A_T}{T} C_T + r_{TQ} \frac{A_Q}{Q} C_Q\right)^2 = \left(\frac{A_T}{T} \frac{L_v}{\rho c_p} \beta + r_{TQ} \frac{A_Q}{Q}\right)^2 C_Q^2,$$

so that the zero in $\frac{\partial C_n^2}{\partial \beta}$ now coincides with C_n^2 = 0 m$^{-2/3}$ so that $C_{n,\min}^2$ = 0 m$^{-2/3}$. The corresponding $\beta_{\max}$ only depends on p, Q and T. Deviations of r_{TQ} from ±1 result in $C_{n,\min}^2 >$ 0 m$^{-2/3}$ (see Figure 2) and higher values of $\beta_{\max}$, so that the safest estimate of the maximum Bowen ratio is that for $r_{TQ} = \pm 1$. For common atmospheric conditions in temperate climates, $\beta_{\max} \ge 2.5$.

[20] If the measured value of C_n^2 is not between $C_{n,\min}^2$ and $C_{n,\max}^2$, it can be concluded that the measurements are not consistent with the inversion model assumptions. This implies that either the assumptions in RWS-EBM are not valid under the given circumstances and/or the measured value of C_n^2 is affected by factors other than the turbulent fluxes (see also section 3.3).

3.2. Sensitivity

[21] In the remainder of this paper, the latent heat flux will be treated as the resulting variable of the RWS-EBM, as this variable is directly related to the evaporation, which is the main focus of this paper. Apart from $R_n - G$, the RWS-EBM is sensitive to C_n^2 and the meteorological variables u and r_{TQ}. Because the effective roughness length z_0 can

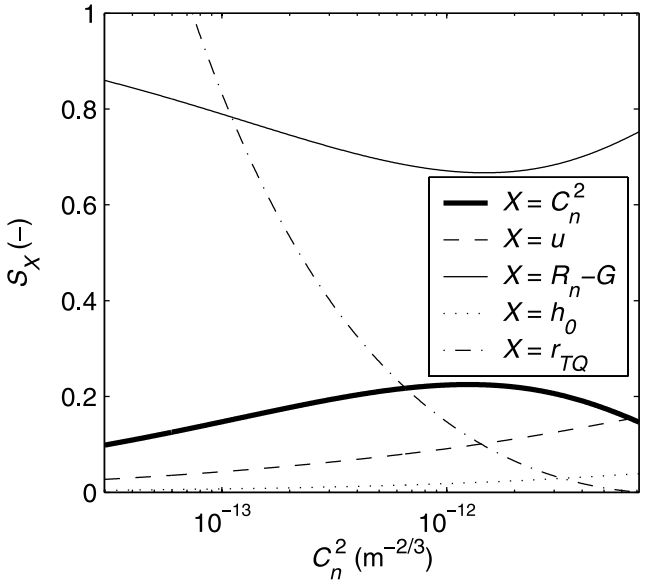

Figure 3. Sensitivity coefficients of L_vE as a function of C_n^2, with $R_n - G = 400$ W m^{-2}, $u = 3.0$ m s^{-1}, $h_0 = 0.5$ m, and $r_{TQ} = 1$.

usually only be roughly estimated, it is important to quantify the effect of uncertainties in h_0 (which is directly linked to z_0 and d_0 through equations (12) and (13), respectively). The method is relatively insensitive to T, Q and p under commonly occurring atmospheric conditions, so that these variables will not be considered here. The degree to which C_n^2, u, $R_n - G$, h_0 and r_{TQ} affect the resulting latent heat flux is analyzed here. The larger the effect, the more important it is to accurately measure or estimate the particular variable.

[22] The sensitivity analysis will be carried out similarly to that of *Andreas* [2000], where the relative change in the resulting variable is expressed in terms of a linear combination of the relative changes in the input variables. If Y is the resulting variable, and X_i ($i = 1,2,\ldots N$) are the N input variables, the relative change in Y can be expressed as

$$\frac{\mathrm{d}Y}{Y} = \sum_{i=1}^{N} S_{X_i}^{(Y)} \cdot \frac{\mathrm{d}X_i}{X_i}, \tag{20}$$

where

$$S_{X_i}^{(Y)} = \frac{X_i}{Y}\left(\frac{\partial Y}{\partial X_i}\right) \tag{21}$$

is defined as the sensitivity coefficient of Y to X_i.

[23] The sensitivity coefficients of L_vE to C_n^2, $R_n - G$, u, h_0 and r_{TQ} have been computed for different values of C_n^2, $R_n - G$, u, h_0 and r_{TQ}, all within a range that is commonly observed. Because the graphs are relatively similar for these different values, Figure 3 (which only shows the sensitivity coefficients as a function of C_n^2 with $R_n - G = 400$ W m^{-2}, $u = 3.0$ m s^{-1}, $h_0 = 0.5$ m, and $r_{TQ} = 1$) may be considered to be illustrative for the entire range of commonly observed values of these variables. The superscript in $S_X^{(L_vE)}$ (equation (21)) is omitted for clarity of notation.

[24] The latent heat flux is most sensitive to the total available energy, which is to be expected because L_vE is directly related to $R_n - G$ (see equations (14) and (15)). This indicates that the RWS-EBM relies heavily on accurate measurements or estimates of $R_n - G$. The other central variable of the RWS-EBM, C_n^2, is also shown to strongly affect L_vE, especially for higher values of C_n^2 (i.e., under relatively wet conditions). This is essential, as the RWS-EBM has been developed based on this sensitivity. The sensitivity of the latent heat flux to the wind velocity u becomes larger as C_n^2 increases, so that it is also important to accurately measure the wind velocity. Because h_0 affects L_vE much less than the other variables, a rough estimate is usually good enough for the RWS-EBM. For high values of C_n^2, the sensitivity of the latent heat flux estimate to r_{TQ} is relatively small, which means that errors in the estimate of this variable will not be very important in this range. This sensitivity becomes much larger for low values of C_n^2, although this is partly caused by the lower values of the resulting L_vE, which is the denominator of $S_{X_i}^{(Y)}$ in equation (21). Therefore correctly estimating r_{TQ} becomes more important during dry conditions (small C_n^2). The effect of errors in r_{TQ} is further discussed in section 3.3.

3.3. Sources of Error

[25] Because there are usually no measurements of r_{TQ} available, we use the assumption that $r_{TQ} = 1$ in the remainder of this paper. *Katul et al.* [1995], using eddy covariance measurements over different terrain types (natural uneven age forest, uniform bare soil and grass-covered pine forest), show that for unstable conditions ($-\frac{z}{L_{Ob}} \leq 1$) values of r_{TQ} increase with increasing $-\frac{z}{L_{Ob}}$ and are typically between 0.4 and 1. Figure 4 shows the absolute (ΔL_vE) and relative errors in the latent heat flux resulting from erroneously assuming $r_{TQ} = 1$ as a function of the actual value of r_{TQ}, for different values of C_n^2. The other variables are held constant at $R_n - G = 400$ W m^{-2}, $u = 3.0$ m s^{-1} and $h_0 = 0.5$ m.

[26] An overestimation of r_{TQ} will always lead to an overestimation of L_vE, which can also be seen in Figure 3, where $S_{r_{TQ}} > 0$. As was concluded in section 3.2, the error resulting from an error in r_{TQ} is lower for high values of C_n^2. Even for significant overestimates of r_{TQ}, the error in the latent heat flux is not extremely large at moderate to large values of C_n^2 (i.e., under relatively wet conditions).

[27] A major source of error in the use of radio wave scintillometers lies in the fact that they are highly sensitive to mechanical oscillations. This means that if either the transmitter or the receiver (or both) is mounted on a structure that vibrates in the wind, the derived C_n^2 values will likely be overestimated [see, e.g., *Meijninger et al.*, 2002b]. The fluctuations in the signal caused by fluctuations in the path-integrated absorption by atmospheric constituents can also contribute considerably to the derived C_n^2 [*Green et al.*, 2001]. Moving scatterers such as trees close to the signal path can scatter part of the beam toward the receiver, in which case the signal fluctuations are again enhanced. Careful positioning of the instrument is therefore very important.

[28] The error in C_n^2 due to these effects is generally positive, so that the latent heat flux will be overestimated using the proposed method. Generally, if such errors occur,

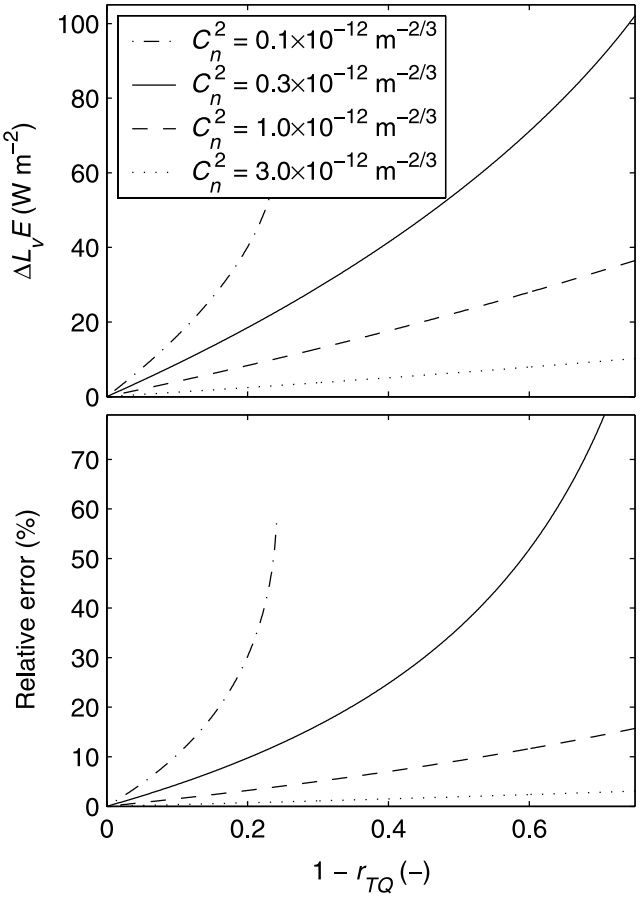

Figure 4. Error in L_vE resulting from a deviation of the actual r_{TQ} from the assumed value of 1 for different values of C_n^2. The line for $C_n^2 = 0.1 \times 10^{-12}$ m$^{-2/3}$ does not go beyond $1-r_{TQ} = 0.24$ (where $\Delta L_vE = 62.8$ W m^{-2}) because otherwise $C_n^2 < C_{n,\min}^2$.

this can be noticed by the fact that the measured C_n^2 may exceed $C_{n,\max}^2$, especially under relatively wet conditions.

4. Experimental Verification

[29] The RWS-EBM will be tested using data collected in the Flevoland field experiment, which will be described in section 4.1. The results will be compared to eddy covariance (EC) measurements and to latent heat fluxes derived from a combination of a RWS and a large-aperture scintillometer (LAS) in section 4.2.

4.1. Flevoland Field Experiment

[30] We have used the processed data set from the Flevoland field experiment as described by *Meijninger et al.* [2002a, 2002b]. This experiment was carried out in the southern part of Flevoland, Netherlands (see Figure 5), between 18 July and 20 August 1998. This was a wet period, in which the evaporation was close to potential most of the time. A 27-GHz scintillometer system with 0.6-m-diameter antennas, manufactured at the Eindhoven University of Technology and on loan from the Horticultural Research Institute of New Zealand [*Green et al.*, 2000, 2001] was used for this experiment. It was mounted on two wind turbines, placed 2.2 km apart, at a height of 10.9 m (both the transmitter and the receiver). The intensity of the receiver signal was band-pass filtered between 0.03 Hz and 20 Hz, and sampled at a rate of 10 Hz. Of this sampled signal, the variance was taken over 30-min periods and recorded. All other measured variables were averaged over the same 30-min periods in this experiment. Because the terrain around the scintillometer is completely flat, the height of the scintillometer above the terrain z_L is constant. For further details concerning this experiment, the reader is referred to the work by *Meijninger et al.* [2002a, 2002b].

[31] The heat fluxes that affect the scintillometer signal originate from rectangular plots with dimensions of approximately 0.5 km, where potatoes, sugar beets, wheat and onions are grown. Figure 5 shows that the spatial distribution of these plots is roughly isotropic (which makes the source distribution roughly independent of the wind direction), and each of the four crop types covers approximately 25% of the total area around the scintillometer. The effective roughness length z_0 was estimated by *Meijninger et al.* [2002a] to be relatively uniform at 0.06 m (so that h_0 = 0.48 m, see equation (12)) over the entire area.

[32] In four of the plots (each with a different crop type), eddy covariance (EC) systems were installed (see Figure 5) to independently measure the heat and momentum fluxes and the correlation coefficient between the temperature and humidity fluctuations. These EC systems were mounted on masts at 4.8 m above the terrain in the sugar beet field, at 3.5 m in the wheat and potato fields, and at 2.8 m in the onion field. Footprint analyses have been conducted by

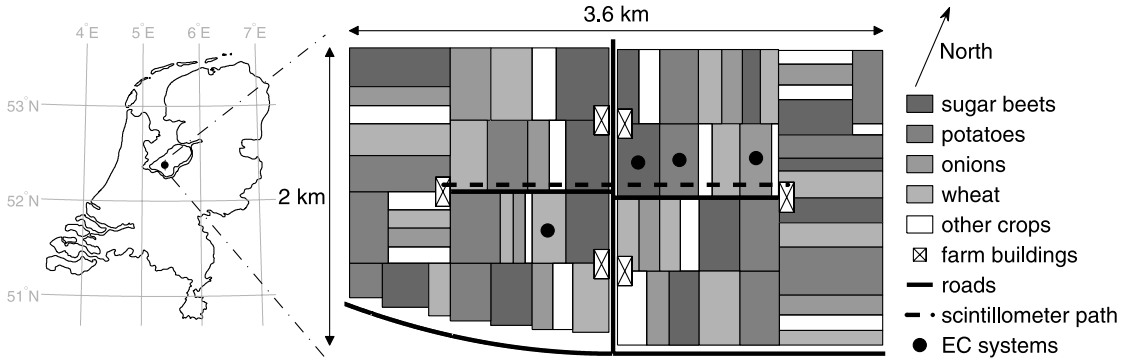

Figure 5. Location of the experimental site within the Netherlands and a land use map of the study area [after *Meijninger et al.*, 2002a].

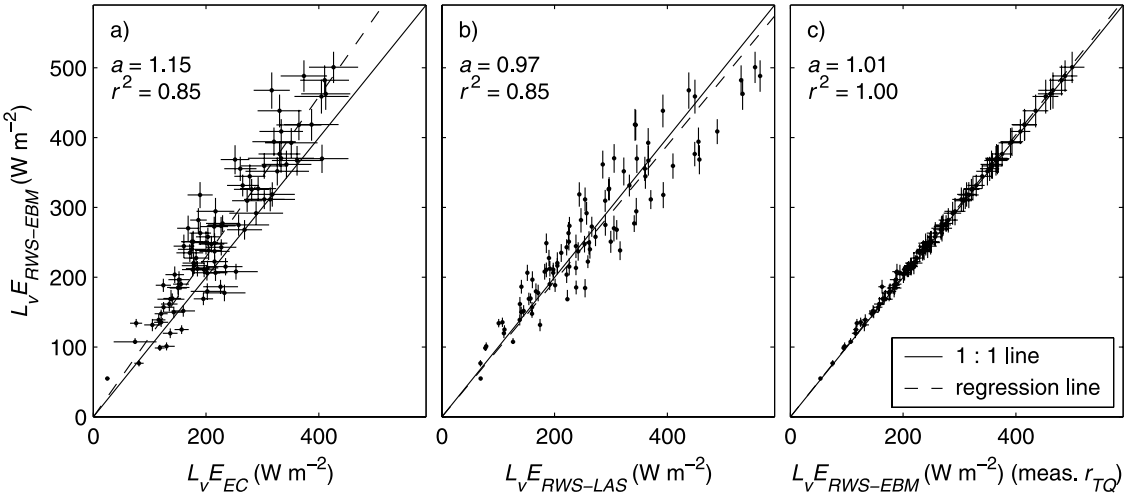

Figure 6. Comparison of the latent heat flux estimated using the RWS-EBM and that estimated using (a) weighted EC measurements, (b) combined RWS and LAS measurements (the two-wavelength method), and (c) the RWS-EBM with r_{TQ} values measured by the EC systems. The slopes of the linear regression lines a and their coefficients of determination r^2 are shown in the top left corners of the graphs.

Meijninger et al. [2002b] to verify whether the fluxes measured by the EC systems were indeed those originating from the respective fields. In addition to these EC measurements, net radiation and ground heat flux were measured at each site. For the energy fluxes measured by the EC systems (L_vE and H_s), the uncertainty is defined as the 95% confidence interval as determined in Appendix A of *Meijninger et al.* [2002a]. The measurement uncertainty in the other heat fluxes (R_n and G) is taken as the 95% confidence interval as given by the manufacturer of the instruments. Weights are assigned to the fluxes measured by the EC systems according to the wind direction and a footprint analysis [*Meijninger et al.*, 2002a]. A weighted average of the latent heat fluxes measured by the EC systems, which differs only slightly from the unweighted average, is used here to compare to the results of the RWS-EBM.

[33] The wind velocity u used in this section was measured at z_u = 3.9 m, and the temperature T and humidity Q were measured at 3.1 m at the sugar beet site. Because there will usually be only one point at which meteorological variables are measured in an operational setting with a stand-alone radio wave scintillometer, the total available energy ($R_n - G$) used in this study is also the one that has been measured at the sugar beet site. The mean value of the spatial standard deviation of $R_n - G$ normalized by its spatial mean is only 6.6%. Therefore the use of only one point measurement will not introduce major errors. The atmospheric pressure was not measured during the Flevoland experiment. We assume it to be constant at a value of p = 101.3 kPa.

[34] In addition to the radio wave scintillometer, a large-aperture infrared (λ = 930 nm) scintillometer (LAS) was mounted on the same wind turbines at a height of 11.6 m by *Meijninger et al.* [2002a, 2002b]. Heat fluxes can be estimated by combining the C_n^2 estimates from the two scintillometers using the so-called two-wavelength method [*Andreas*, 1989]. In this method, equation (2) is used twice (with different values of C_n^2, A_T and A_Q for the two wavelengths) in combination with equation (5) (again representing two equations) to solve the four unknowns (C_T^2, C_Q^2, H_s and L_vE). Hence the RWS-LAS method is independent of the measured total available energy. The latent heat flux resulting from the RWS-EBM will be compared to this RWS-LAS two-wavelength heat flux as well.

4.2. Results

[35] The scintillometer data used in the comparison are those recorded during daytime (between 9:00 and 18:00) for which measurements of u, R_n, G, T and Q are available at the sugar beet site. *Meijninger et al.* [2002b] have made an additional selection based on visual inspection of the time series of their resulting values of L_vE compared to those measured by the EC systems. Unrealistically high values were found to be caused by mechanical oscillations of the microwave link system setup (which was physically connected to wind turbines) due to wind, and have been discarded. This additional selection indeed removes most of the occurrences of measured C_n^2 values exceeding $C_{n,\max}^2$. Therefore the data points that were used by *Meijninger et al.* [2002b] are employed in the current analysis as well. The resulting data set consists of 92 30-min intervals.

[36] Figure 6 shows the comparison of the latent heat fluxes derived from the RWS-EBM with r_{TQ} = 1 ($L_vE_{RWS-EBM}$) to the weighted EC measurements (L_vE_{EC}), the RWS-LAS two-wavelength method ($L_vE_{RWS-LAS}$), and the RWS-EBM with measured values of r_{TQ}. In this last analysis, over 90% of the values of r_{TQ} exceed 0.5, and approximately 67% are greater than 0.75. The lower values of r_{TQ} occur at low values of $R_n - G$, so that the absolute error in L_vE caused by assuming r_{TQ} = 1 is smaller than expected from Figure 4. The error bars in the RWS-EBM results are solely caused by errors in $R_n - G$, as no error estimates for C_n^2 and the other variables were available. This is also the reason why no error bars are shown for the RWS-LAS analysis. A linear regression has been performed for each of the flux comparisons, and the resulting slopes a and coefficients of determination r^2 are given in the graphs.

[37] The RWS-EBM seems to overestimate the latent heat flux when compared to the latent heat flux measured by the

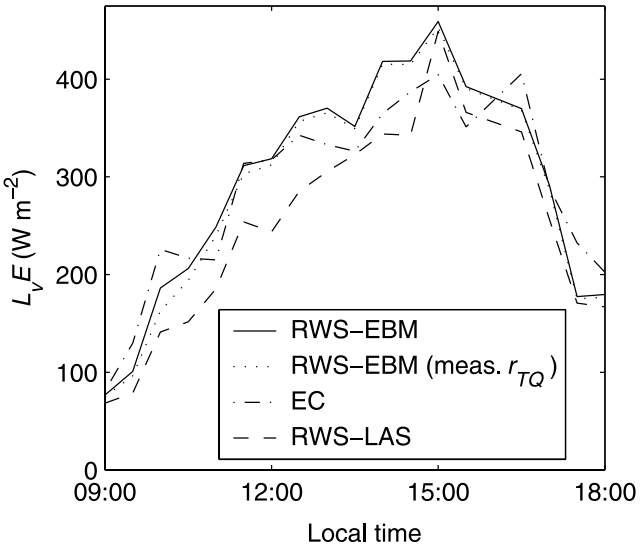

Figure 7. Time series of the latent heat fluxes determined using different methods on 27 July 1998.

EC systems (a = 1.15). However, the sum of the sensible and latent heat fluxes measured by the EC systems does not close the energy budget, whereas the RWS-EBM closes the energy budget by definition. Least squares estimation of a in $R_n - G = a(L_vE + H_s)$ using the fluxes measured by the EC systems gives a = 1.13, with a coefficient of determination r^2 = 0.90. This nonclosure of the EC-derived energy budget explains the apparent overestimation by the RWS-EBM. The high coefficient of determination (r^2 = 0.85) indicates that the RWS-EBM captures the dynamics correctly (85% of the variance explained). The comparison of the RWS-EBM to the RWS-LAS two-wavelength method, with a = 0.97 and r^2 = 0.85 leads to the same conclusion, although this evidence is less strong as the two methods are not independent. The major advantage of the RWS-EBM over RWS-LAS is that only one scintillometer is needed in the former (with additional measurements of $R_n - G$), whereas two are needed in the latter. The third comparison is not meant as a verification of the method but more as an analysis of the effect of the assumption that r_{TQ} = 1 for real data. It is clear from this comparison that the effect of $r_{TQ} < 1$ is very small compared to the size of the error bars (which are solely caused by errors in $R_n - G$).

[38] Figure 7 shows the evolution of the latent heat fluxes of Figure 6 on 27 July 1998. This day was chosen because it was the only day for which data were continuously available. It can be seen that the latent heat fluxes estimated using the different methods are similar, which again leads to conclusion that the RWS-EBM reasonably captures the evaporation dynamics during the Flevoland experiment.

5. Conclusions

[39] A method has been presented that uses radio wave scintillometer measurements in combination with measurements of the total available energy to estimate the latent heat flux, and hence the evaporation: the radio wave scintillometry-energy budget method (RWS-EBM). It has been demonstrated that given the meteorological conditions and assuming the Monin-Obukhov similarity theory to be valid, the range of physically possible values of C_n^2 is limited. Measured values that exceed $C_{n,\max}^2$ may indicate measurement errors. The method is best suited for relatively wet conditions, as the RWS is most sensitive to humidity fluctuations. If conditions become too dry, the nonuniqueness of the solution of the system of equations may become important, so that an incorrect flux may be estimated.

[40] Sensitivity analyses indicate that it is important to accurately measure or estimate the total available energy $R_n - G$ and the wind velocity u in order to obtain reliable estimates of the latent heat flux. The fact that r_{TQ} is often unknown in an operational setting is found to be unimportant in wet conditions, although uncertainties in r_{TQ} can cause larger errors in the resulting latent heat flux during dry conditions. This is a second reason why this method (and the use of RWS in general) is most suitable for use in relatively wet conditions, up to Bowen ratio values of $\beta \approx 2$.

[41] The application of RWS-EBM to experimental data collected in southern Flevoland, Netherlands in the summer of 1998 yields good results when compared to independent EC measurements of the latent heat flux and to results of the RWS-LAS two-wavelength method. The errors caused by the assumption that r_{TQ} = 1 are shown to be very small for these data. It can be concluded from these experimental results that the proposed method works well, at least for relatively wet conditions. More experimental research needs to be done to investigate the performance of the RWS-EBM under drier conditions.

[42] **Acknowledgments.** The authors would like to thank colleagues at the Meteorology and Air Quality Group, Wageningen University, in particular W. M. L. Meijninger, and W. Kohsiek (KNMI) for providing the data that were used to test the method presented in this paper (collected in a project financially supported by the Dutch Technology Foundation STW, project number WMO4133) and for the fruitful discussions. H.L. and R.U. are financially supported by the Netherlands Organization for Scientific Research (NWO) through a grant (016.021.003) in the framework of the Innovational Research Incentives Scheme (Vernieuwingsimpuls).

References

Andreas, E. L. (1988), Estimating C_n^2 over snow and sea ice from meteorological data, *J. Opt. Soc. Am. A Opt. Image Sci.*, *5*, 481–495.

Andreas, E. L. (1989), Two-wavelength method of measuring path-averaged turbulent surface heat fluxes, *J. Atmos. Oceanic Technol.*, *6*, 280–292.

Andreas, E. L. (2000), Obtaining surface momentum and sensible heat fluxes from crosswind scintillometers, *J. Atmos. Oceanic Technol.*, *17*, 3–16.

Bastiaanssen, W. G. M. (2000), SEBAL-based sensible and latent heat fluxes in the irrigated Gediz basin, Turkey, *J. Hydrol.*, *229*, 87–100.

Bastiaanssen, W. G. M., M. U. D. Ahmad, and Y. Chemin (2002), Satellite surveillance of evaporative depletion across the Indus Basin, *Water Resour. Res.*, *38*(12), 1273, doi:10.1029/2001WR000386.

Brutsaert, W. (1982), *Evaporation into the Atmosphere*, 299 pp., Springer, New York.

Businger, J. A., J. C. Wyngaard, Y. Izumi, and E. F. Bradley (1971), Flux-profile relationships in the atmospheric surface layer, *J. Atmos. Sci.*, *28*, 181–189.

de Bruin, H. A. R. (2002), Introduction: Renaissance of scintillometry, *Boundary Layer Meteorol.*, *105*, 1–4.

Green, A. E., S. R. Green, M. S. Astill, and H. W. Caspari (2000), Estimating latent heat flux from a vineyard using scintillometry, *Terr. Atmos. Oceanic Sci.*, *11*, 525–542.

Green, A. E., M. S. Astill, K. J. McAneney, and J. P. Nieveen (2001), Path-averaged surface fluxes determined from infrared and microwave scintillometry, *Agric. For. Meteorol.*, *109*, 233–247.

Hill, R. J., and S. F. Clifford (1981), Contribution of water vapor monomer resonances to fluctuations of refraction and absorption for submillimeter through centimeter wavelengths, *Radio Sci.*, *16*(1), 77–82.

Hill, R. J., S. F. Clifford, and R. S. Lawrence (1980), Refractive-index and absorption fluctuations in the infrared caused by temperature, humidity and pressure fluctuations, *J. Opt. Soc. Am.*, *70*(10), 1192–1205.

Katul, G. G., S. M. Goltz, C.-I. Hsieh, Y. Cheng, F. Mowry, and J. Sigmon (1995), Estimation of surface heat and momentum fluxes using the flux-variance method above uniform and non-uniform terrain, *Boundary Layer Meteorol.*, *74*, 237–260.

Kohsiek, W., and M. H. A. J. Herben (1983), Evaporation derived from optical and radio-wave scintillation, *Appl. Opt.*, *22*(17), 2566–2570.

Leijnse, H., R. Uijlenhoet, and J. N. M. Stricker (2007), Hydrometeorological application of a microwave link: 2. Precipitation, *Water Resour. Res.*, *43*, W04417, doi:10.1029/2006WR004989.

Meijninger, W. M. L., O. K. Hartogensis, W. Kohsiek, J. C. B. Hoedjes, R. M. Zuurbier, and H. A. R. de Bruin (2002a), Determination of area-averaged sensible heat with a large aperture scintillometer over a heterogeneous surface—Flevoland field experiment, *Boundary Layer Meteorol.*, *105*, 37–62.

Meijninger, W. M. L., A. E. Green, O. K. Hartogensis, W. Kohsiek, J. C. B. Hoedjes, R. M. Zuurbier, and H. A. R. de Bruin (2002b), Determination of area-averaged water vapour fluxes with large aperture and radio wave scintillometers over a heterogeneous surface—Flevoland field experiment, *Boundary Layer Meteorol.*, *105*, 63–83.

Parlange, M. B., W. E. Eichinger, and J. D. Albertson (1995), Regional scale evaporation and the atmospheric boundary layer, *Rev. Geophys.*, *33*(1), 99–124.

Pope, S. B. (2000), *Turbulent Flows*, 771 pp., Cambridge Univ. Press, New York.

Su, Z. (2002), The Surface Energy Balance System (SEBS) for estimation of turbulent heat fluxes, *Hydrol. Earth Syst. Sci.*, *6*(1), 85–99.

Tatarskii, V. I. (1971), *The Effects of the Turbulent Atmosphere on Wave Propagation*, translated from Russian, 472 pp., Isr. Program for Sci. Transl., Jerusalem.

Wieringa, J. (1992), Updating the Davenport roughness classification, *J. Wind Eng. Ind. Aerodyn.*, *41*, 357–368.

Wyngaard, J. C., Y. Izumi, and S. A. Collins, Jr. (1971), Behavior of the refractive-index-structure parameter near the ground, *J. Opt. Soc. Am.*, *61*(12), 1646–1650.

H. Leijnse, J. N. M. Stricker, and R. Uijlenhoet, Hydrology and Quantitative Water Management, Wageningen University, Droevendaalsesteeg 4, 6708 PB Wageningen, Netherlands. (hidde.leijnse@wur.nl)